Quasi-Periodic Oscillations in a Symmetric General Circulation Model

B. N. GOSWAMI[1] AND J. SHUKLA

NASA/Goddard Laboratory for Atmospheric Sciences, Goddard Space Flight Center, Greenbelt, MD 20771

(Manuscript received 13 December 1982, in final form 25 August 1983)

ABSTRACT

Long time integrations with a symmetric version of the GLAS Climate Model with hydrology have shown that the Hadley circulation has well defined strong and weak episodes. This oscillation of the Hadley circulation seems to occur in two dominant range of periodicities, one with periods between 10 and 15 days and another with periods between 20 and 40 days. This quasi-periodic behavior of the Hadley circulation is seen only when the moist convective heating is determined by dynamics. If the latent heating in the atmosphere is prescribed and kept artificially fixed, this oscillation of the Hadley circulation disappears. Thus, this oscillation of the Hadley circulation appears as a result of interactions between moist convective and dynamical processes.

A wave phenomenon is seen in the lower atmosphere that propagates toward the position of maximum radiative heating. This wave perturbation has a length scale of about 15–20 degrees latitude in the north–south direction. This phenomenon has large amplitude over land and relatively small amplitude over the oceans. It is found that evaporation from the land surface plays a key role in generation and maintenance of this phenomenon. In a controlled experiment in which evaporation from the land surface was kept zero, this wave perturbation in the lower atmosphere was not observed. The relevance of these phenomena to observed low-frequency fluctuations in the tropics and to the transient behavior of the Intertropical Convergence Zone is discussed.

1. Introduction

During the past several years observational evidence has been presented (Madden and Julian, 1971, 1972; Yasunari, 1979, 1980, 1981; Sikka and Gadgil, 1980; Krishnamurti and Ardanuy, 1980) for the existence of quasi-periodic fluctuations of the tropical circulation with periods around two weeks and around 40 days. Understanding the mechanisms of these quasi-periodic oscillations in the tropical atmosphere is expected to improve the predictability of the short range climate fluctuations in the tropics.

Madden and Julian (1971) first showed the existence of the oscillations with period around 40 days. They examined nearly ten yers of observations for zonal winds and surface pressure at one tropical station (Canton Island, 3°S, 172°W). By using spectral analysis of the time series for these fields, they showed the existence of a predominant peak in the spectrum with periods between 40 and 50 days. In a subsequent study (Madden and Julian, 1972) they examined similar data at a large number of tropical and subtropical stations. Spectral and cross-spectral analysis of the data showed that this oscillation is present in most of the tropical stations. They also found that the amplitude of this oscillation is large for the tropical stations and, in general, small for the subtropical stations. Using Canton Island as the reference station, they calculated cross spectra and coherence-squares of the surface pressures of a large number of tropical stations. The coherence-square for most of the stations with respect to the reference station were found to be above background at 95% level. This indicated that almost all of these stations were affected by the same phenomenon. The phase angles at different stations showed a propagating character for the oscillation from west to east. They estimated that it took approximately 3 days for the disturbance to move from Singapore (1°N, 104°E) to Canton (3°S, 172°W) and another 3 days to reach Balboa (9°N, 80°W). Thus, they concluded that this oscillation is, by and large, confined to the tropics and is of large scale in nature.

Recent studies by Sikka and Gadgil (1980) and Yasunari (1979) show some very interesting transient features of the Intertropical Convergence Zone (ITCZ) over the Indian ocean and the Southeast Asian region. Sikka and Gadgil (1980) studied the daily variation of the Maximum Cloud Zone (MCZ) and the 700 mb trough over the Indian longitudes 70–90°E and between the equator and 35°N during April–October for the period 1973–77. They found that during June–September two MCZs exist in this region—one over the continents and the other over the oceans. They also observed that both MCZs exhibit epochs of strong and weak intensity. The strong episodes of the continental MCZ was shown to be related to the weak episodes of the oceanic MCZ and vice versa. Moreover, they noted that both MCZs have a northward propagation in time. Yasunari (1979), using 122 days cloud pictures from NOAA-2 satellite during 1 June–30 Sep-

[1] Present affiliation: Center for Atmospheric and Fluid Sciences, Indian Institute of Technology, Hauz Khas, New Delhi, 110019, India.

tember 1973, found quite similar features of the MCZ. This study also showed the existence of two MCZs and their northward propagation. The data used in this study covered the Eastern Hemisphere between 0°E and 180°E and 35°S–40°N. Yasunari (1979) carried out a spectral analysis of the digital cloud intensity in the visible range and showed that the cloudiness fluctuations have two dominant periodicities—one around 15 days and another around 40 days. The 40 day oscillation showed marked northward movement in the Asian monsoon area from the equatorial region to about 30°N and a southward movement over Africa and the central Pacific. The 15 day oscillation also showed northward propagation in the Asian monsoon region.

In later studies, Yasunari (1980, 1981) used geopotential and wind data from a large number of stations over India, Thailand, Malaysia, Singapore and Gan Island for the period between June–September 1969 and studied in detail the horizontal and vertical structure of the 40 day period. The zonal winds show northward propagation both at 850 mb as well as 200 mb. The geopotential height at 850 mb also showed northward movement in the Indian region. In contrast, the geopotential height at 200 mb over the Indian region showed a standing oscillation.

In the Indian region, the existence of an oscillation with period about 15 days during the monsoon season has been documented in several other studies (Keshavamurty, 1973; Krishnamurti and Bhalme, 1976; Murakami, 1976; Krishnamurti and Ardanuy, 1980). All these studies indicate that the active and break epochs of the South Asian summer monsoon have some relation to this oscillation of the tropical circulation with period around 15 days. Yasunari (1981) showed that even the 40 day oscillation has some relation to the active and break epochs of the South Asian summer monsoon. He used two band pass filters having peak response with periods around 14 and 40 days on the geopotential field during June–September 1969. It was seen that all the monsoon depressions during that season occurred during the troughs of the filtered geopotential field for both the oscillations.

In a recent study Krishnamurti and Subrahmanyam (1982) analyzed the wind field at 850 mb during the summer monsoon experiment (MONEX). They extracted the 30–50 day wind component using a band pass filter. The filtered wind field showed the steady northward propagation of a train of troughs and ridges. Three major storms during the MONEX were noted to form within the trough line of this system. Thus, there is a good deal of evidence that the tropical circulation exhibits temporal fluctuations with two dominant ranges of periodicities, one with period around 15 days and another with period around 40 days. Moreover, there is some evidence that these fluctuations have northward or southward propagation at different regions. Madden and Julian (1972) and Yasunari (1981) have documented that these oscillations are extremely large scale in nature in the zonal direction. In a recent study, Anderson and Rosen (1983) used zonally averaged zonal winds for five years and showed that the 40–50 day oscillation originates in the tropical upper troposphere and propagates downward and poleward. This feature of these oscillations suggests that it may be possible to understand these oscillations with a zonally averaged model.

As to the origin of these oscillations in the tropical atmosphere there has been mostly speculation and to our knowledge only one numerical simulation study (Webster and Chou, 1980a,b). Regarding the origin of the 15 day oscillation, Misra (personal communication, 1975) and Krishnamurti and Bhalme (1976) had suggested that it may be due to cloud–radiation feedback processes. As for the origin of the 40-day oscillation, Madden and Julian (1972) proposed that it may be due to a large scale wave travelling in the east-west direction. Yasunari (1981) tried to explain the northward propagation of the 40 day oscillation in the South Asian summer monsoon region as being triggered by cold- (or warm) air outbreaks from Southern Hemisphere. Most of these explanations are speculative in nature and have not been confirmed by theoretical and numerical studies. Stevens (1982) recently examined the stability of zonal flows near the equator to symmetric perturbations. He suggested that a symmetric inertial instability may be responsible for the 40–50 day oscillation in the tropics. Only in recent studies by Webster and Chou (1980a,b), integrations of a numerical model presented some evidence regarding the low frequency transitions in the tropics. They used a coupled system of a zonally symmetric two-layer nonlinear global primitive-equation atmospheric model and a mixed-layer ocean model. They found in an experiment in which the lower boundary had distributions of land and ocean and in which the hydrological processes were included, that orderly periods of strong and weak epochs occur during the Northern Hemisphere summer. These episodes were seen in the surface temperature field as well as the precipitation field. These epochs of strong and weak intensity have a period of about two weeks and they are found to have a northward propagation. These low frequency transitions were not seen in the dry experiments. The authors suggested that these transitions occur as a result of interaction between hydrology over the heated land mass to the north and the ocean to the south. However, it is not very clear from this study why the period of these transitions is about two weeks and why they move northwards.

The present study, which uses the symmetric model, was not initiated with a specific goal of understanding the low frequency oscillations in the tropical atmosphere. Rather, this study evolved as an outgrowth of

another investigation (Goswami *et al.*, 1984; hereafter referred to as GSSS) in which we observed remarkable oscillations of the Hadley circulation for an ocean covered earth. We do not wish to imply that the observed 15 and 40 day oscillations are symmetric, but only to show that interactions between dynamics and moist convection can produce fluctuations in this time range. We found the simulations to be of sufficient interest and importance that in order to understand the nature of these oscillations in the model atmosphere, we carried out several more controlled experiments and analyzed the results in detail. A list of these experiments with brief description is presented in Table 1.

Analyses of results from these experiments show that the simulated tropical Hadley cell displays episodes of strong and weak intensity. Spectral analysis reveal two dominant ranges of periodicities, one with periods around 10–15 days and another around 20–40 days. These oscillations of the simulated tropical circulation are in some respects similar to the observed oscillations of the tropical atmosphere (Madden and Julian, 1971, 1972; Yasunari, 1979, 1980, 1981; Sikka and Gadgil, 1980). The model simulations also show a northward propagation of the precipitation field and of other fields in the lower atmosphere very similar to the northward propagation observed by Sikka and Gadgil (1980) and Yasunari (1979) in the cloud pictures and by Yasunari (1980, 1981) in the geopotential field and zonal winds at 850 mb.

The quasi-periodic oscillations of Hadley circulation are seen only when the moist convective heating is determined by dynamics. If the latent heating is prescribed and kept constant in time, these oscillations of the tropical atmosphere disappear. This indicates that the quasi-periodic fluctuations in the model atmosphere result due to interactions between moist convective and dynamical processes. Further analysis shows that the moist convective processes modify the tropical atmosphere in such a way that at a later time it becomes neutral to conditional instability. This slows the moist convective activity. At a still later time, the dynamics brings the atmosphere back to a conditionally unstable regime, and moist convection again starts.

Our analyses also suggest that the wave perturbation in the north–south direction and its northward propagation seen in the precipitation and other fields in the lower atmosphere could be a surface induced phenomenon. It is shown that the fluctuations in the latent heat of evaporation from the surface maintains this phenomenon. In a controlled experiment in which evaporation from the land surface is kept zero, these wave perturbations are not seen. Moreover, the amplitude of this wave perturbation is larger over land as compared to that over the ocean. For example, the amplitude of the surface air temperature perturbation seems to propagate towards the position of maximum radiative heating. For the controlled spring simulation

TABLE 1. Brief description of various experiments discussed in this study.

Experiment	Description	Length of integration (days)
I	Moist Ocean, Equinox (MOE) run Permanent equinox condition, global ocean	150
II	Moist Ocean, Summer (MOS) run Permanent summer solstice condition, global ocean	150
III	Fixed Soil Moisture, Summer (FSMS) run Permanent summer solstice, global land, flat topography	600
IV	Fixed Soil Moisture, Equinox (FSME) run Permanent equinox condition, global land, flat topography	150
V	Variable Soil Moisture, Summer (VSMS) run Permanent summer solstice condition, global land, flat topography	150
VI	No Soil Moisture, Summer (NSMS) run Permanent summer solstice condition, global land, flat topography	180

in which the position of the sun is kept fixed over the equator, the wave perturbations seem to propagate from north and from south toward the equator. For the permanent summer solstice simulation, the wave perturbations are seen to propagate from south to about 20–25°N. However, the exact dynamical reason for the propagation of these perturbations is not clear from our analysis. In any case, this study for the first time simulates the quasi-periodic oscillations of the tropical atmosphere and their propagation characteristics in the lower atmosphere and indicates the dynamical origin of these phenomena.

The model used in this study is the symmetric version of the GLAS Climate Model described in detail in an earlier paper (Goswami *et al.*, 1984). This is a global nonlinear primitive-equation model. It uses 9 level σ-coordinates in the vertical and a 4° latitude grid in the north–south direction. The model also uses all of the physical parameterizations used in the GLAS Climate Model including radiative and moist convective processes and the ground hydrology. Thus, the model used in this study has much better resolution in the vertical and it uses more sophisticated parameterizations for the physical processes as compared to those for the model used by Webster and Chou (1980a,b). On the other hand, unlike Webster and Chou (1980a,b), we do not have an interactive ocean. In our model, whenever the lower boundary is ocean, a sea surface temperature (SST) is prescribed and kept fixed. However, the results from our experiments indicate that, an interactive ocean is not crucial either for the

transient oscillations of the tropical atmosphere or for the northward propagation of these oscillations.

2. The results

In this section we shall present evidence of the two phenomena described in Section 1, namely, 1) the episodic behavior of the tropical circulation in general and 2) propagation characteristics of these oscillations in the lower atmosphere. For this purpose we shall present results of six different experiments. These experiments correspond to different boundary conditions (land or ocean) with hydrology including or excluding certain surface processes (e.g., soil moisture). For convenience of referring in the text, these experiments are described briefly in Table 1 and an acronym is given to each experiment for future reference. No mountains are included in these experiments. All the experiments described briefly in Table 1 are global runs with hydrology. For the runs with all ocean lower boundary, we prescribed a sea surface temperature (SST) and kept it fixed. The SST distribution used for the summer run and equinox run are same as those used in GSSS. To facilitate easy reference for the reader we show this SST distribution again in Fig. 1.

As in GSSS, we have used a relatively large value for the coefficient of the vertical eddy viscosity for all the runs described in Table 1. This is done in order to make sure that our symmetric model does not become unstable to symmetric perturbations. The vertical eddy viscosity used in this study is such that the coefficient of the vertical eddy viscosity in the middle layer of our model is about 33 $m^2 s^{-1}$. The coefficient of the vertical eddy viscosity in our model decreases linearly with pressure. We also discussed in GSSS that the cloud-radiation feedback process in the symmetric model results in unrealistic sources and sinks of heat.

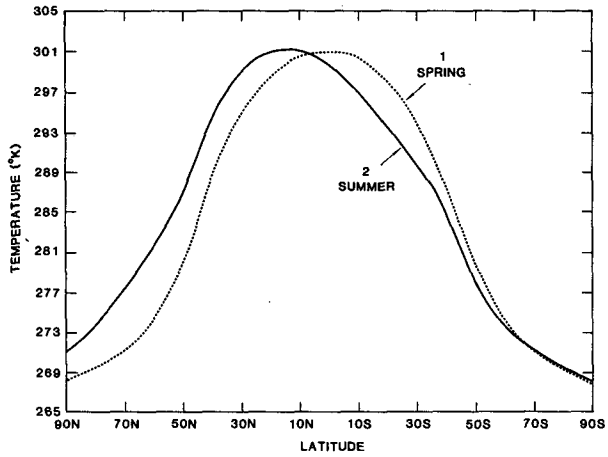

FIG. 1. Sea surface temperature prescribed for the all-ocean runs. Curve 1 corresponds to the equinox condition and curve 2 corresponds to the Northern Hemisphere summer condition.

Therefore, as was done in GSSS, we have suppressed the cloud-radiation feedback process for all the runs discussed here. A climatological distribution of moisture was prescribed and kept fixed for the radiative calculations. This was done so that elimination of one more interactive process would make it easier to understand the results. We repeated, however the summer run with fixed soil moisture (run III), letting the atmospheric moisture interact with radiation dynamically. Although, we are not going to present the results of this run, we would like to emphasize that inclusion of this process does not change the qualitative nature of the results. For the fixed soil moisture runs, the soil moisture for the land was kept fixed at 30% of the maximum available field capacity.

In the next few sections we shall present results from the experiments shown in Table 1. Time evolution of various fields are shown between 50°S and 50°N. As we do not include the effect of the large scale eddies in this version of our symmetric model, it essentially simulates the Hadley circulations in the tropics and does not simulate the Ferrel cells. Therefore, the fluctuations of the circulation north of 50°N and south of 50°S are very small. This is why we shall present the time evolution of the circulation between 50°S and 50°N.

All the latitude–time sections presented in this paper were first plotted using the digital output. We encountered some problems in plotting the contours of the precipitation field using the programs available to us. This is due to the fact that the latitude–time array for the precipitation field appears as discontinuous "blobs". In order to overcome this difficulty, we used a nine-point smoothing on the latitude–time array of the precipitation field before plotting. This results in a damping of the precipitation episodes and gives the impression of a background precipitation in some cases. We would like the reader to keep this in mind in interpreting the latitude–time sections of the precipitation fields.

a. All ocean runs

In this section, we present the results of two experiments with all-ocean lower boundary. These two experiments are the very same experiments discussed in Section 3 of GSSS. All the physical processes including the moist convective heating are calculated by using the parameterization of the GLAS Climate Model described in section 2 of GSSS. In the first experiment, the prescribed SST is symmetric about the equator (curve 1 of Fig. 1). The SST distribution roughly corresponds to the spring condition. The position of the sun, in this experiment, is kept fixed over the equator. In the second experiment, the prescribed SST has a maximum at about 18°N (curve 2 of Fig. 1). This SST distribution roughly corresponds to the Northern

Hemisphere summer condition. The position of the sun in this case is kept fixed at 23.5°N.

Both experiments described above were integrated for about 150 days of simulation time. In order to see the temporal evolution of the circulation, we present time series of the last 90 days of the daily averaged precipitation, surface air temperature, stream function at level 5 (505 mb) and streamfunction at level 2 (175 mb) in Fig. 2 for the summer run with sun fixed over 23.5°N and SST having a maximum around 18°N (experiment II). The time series of the precipitation in the experiments show that the maximum precipitation occurs in a band around the SST maximum. However, there are strong and weak episodes of the precipitation. The surface air temperature shows only small fluctuations in the region of maximum precipitation. The streamfunction at level 5 also shows the strengthening and weakening episodes suggested by the precipitation field. The episodic behavior of the circulation is more prominent in the streamfunction field at level 2. The streamfunction at level 5 as well as the one at level 2 show, however, that although fluctuations exist in the mass flux in the Hadley cell, the position of the ITCZ, in general, remains over the SST maximum.

The time series of the daily averaged precipitation, surface air temperature, streamfunction at level 5 and the one at level 2 for the all-ocean equinox run (experiment I) show qualitatively the same behavior as those for the summer run. For this run, the SST is symmetric about the equator with the maximum over the equator. The streamfunction field again shows the strengthening and weakening episodes. However, in this case the region of maximum convergence and hence the position of the ITCZ remains more or less steady around 2°S. For the all-ocean summer run (Fig. 2) we note that the mass flux of the Hadley cell in the Southern Hemisphere is much larger than those in the Northern Hemisphere Hadley cell. However, for the all-ocean equinox run the mass fluxes of the Hadley cells in both hemispheres are comparable. As the result for the equinox run is qualitatively similar to those for the summer run, we shall not show the time series for the equinox run.

From both of these runs it is seen that, although the Hadley cells show the episodic behavior in time, the position of the ITCZ remains close to the region of SST maximum. In GSSS, we have shown that the ITCZ occurs in the region of the SST maximum because a deep heat source is dynamically generated in this region.

The most striking feature seen in Fig. 2 is the episodic behavior of the Hadley circulation. In order to gain some insight into the origin of these oscillations of the Hadley circulation, we examined the time series of the streamfunction field for an experiment in which the moist convective heating is constrained to remain constant with time. This experiment was described in Section 4 of GSSS and corresponds to Northern Hemisphere summer condition. For this experiment, the latent heating field was prescribed from observed zonally averaged precipitation and kept fixed with time of integration. The upper panel of Fig. 3 shows the time series of the daily averaged streamfunction at level 5 (505 mb) for this run. This figure shows that after initial adjustments, the model atmosphere reaches an absolutely steady state. For direct comparison, the daily averaged streamfunction at level 5 (505 mb) for the all-ocean summer run in which the latent heating is determined by dynamics (ψ_5 of Fig. 2) is shown in the lower panel of Fig. 3. Fig. 3 clearly shows that the oscillations of model tropical atmosphere are related to the oscillations of the moist convective processes. In Section 3 we shall present more evidence supporting this conclusion.

b. All land runs: No mountain

1) FIXED SOIL MOISTURE RUNS

In this section we shall present results of two runs with an all-land lower boundary. One of these runs corresponds to a permanent equinox with sun fixed over the equator (experiment IV) while the other experiment corresponds to a permanent summer solstice with sun fixed over 23.5°N (experiment III). For reasons discussed in GSSS, we did not include the cloud–radiation feedback and we prescribed a climatological mean moisture distribution for radiative calculations. We also kept the soil moisture fixed for these runs. The prescribed ground wetness for these runs at all latitudes is 30% of the maximum available field capacity. For both runs, the model was integrated for more than 150 days.

Figure 4 shows the time series of the last 90 days of integration of the daily averaged precipitation, the surface air temperature, the streamfunction at level 5 and the one at level 2 for the fixed soil moisture summer run. The time series of the same quantities for the fixed soil moisture equinox run are shown in Fig. 5. The time series of these quantities show some very interesting features. At a given latitude in tropics and subtropics, all the fields show episodes of strong and weak periods in both the runs. The precipitation, the surface temperature and the streamfunction at the lower atmosphere (not shown here) show a wave pattern in the north–south direction. However, the streamfunction at level 5 and that at level 2 do not show this wave pattern. Thus, this wave perturbation is essentially confined to the lower atmosphere. This wave perturbation has a scale length between 15 and 20° latitude. In the equinox run (Fig. 5), this wave perturbation moves northward from the Southern Hemisphere to the equator and moves southward from the Northern Hemisphere toward the equator. The

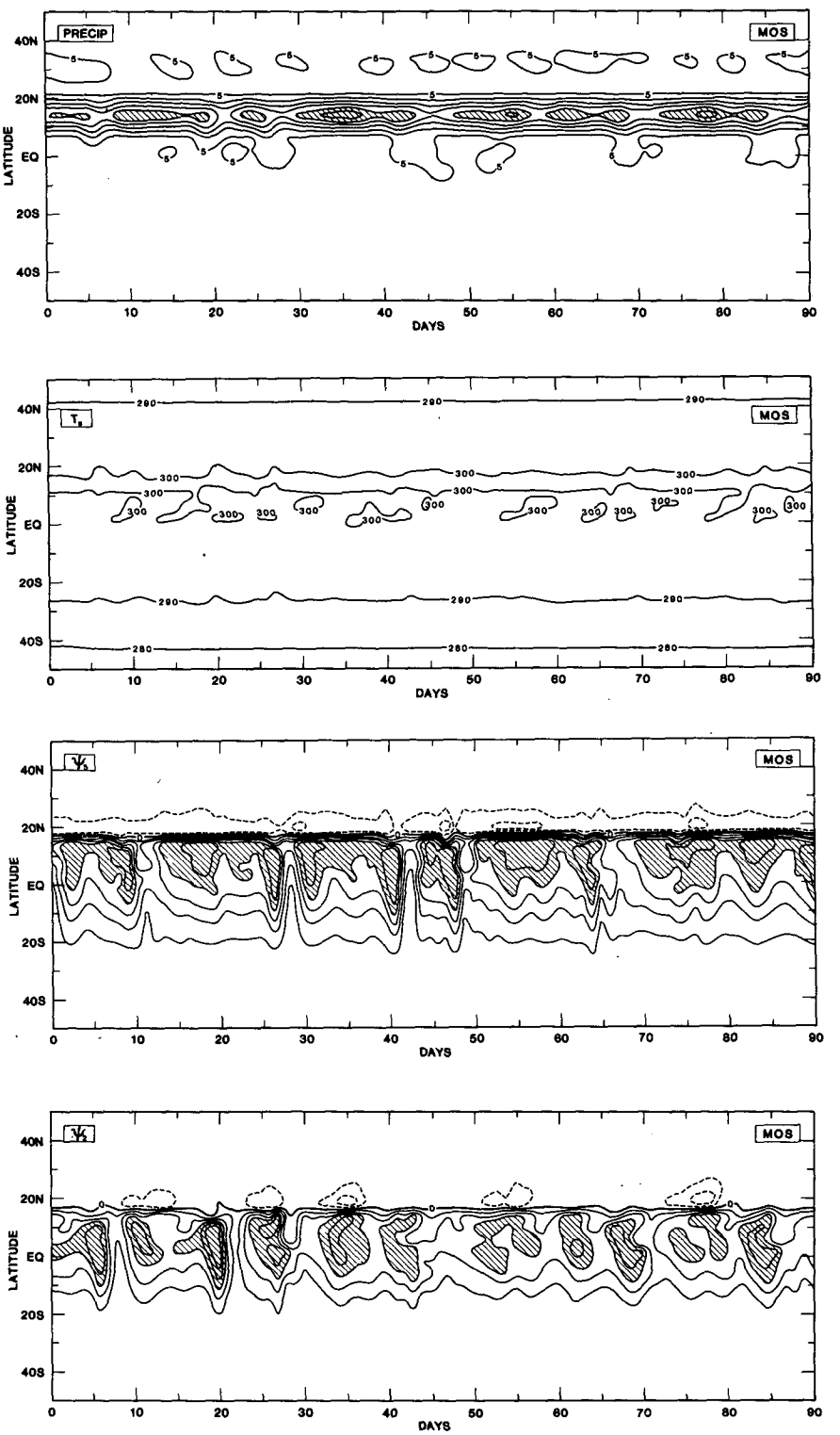

FIG. 2. Time series of precipitation (P), surface air temperature (TS), streamfunction at 505 mb (ψ_5) and streamfunction at 175 mb (ψ_2) for the all-ocean summer run (MOS). Units: P (mm day^{-1}), TS (K), ψ (10^{10} g s^{-1}). Contour interval for P, is 10, for TS is 10, for ψ_5 is 20 and for ψ_2 it is 10. For P, contours greater than 45 are shaded, for ψ_5 contours greater than 80 are shaded while for ψ_2, contours greater than 30 are shaded.

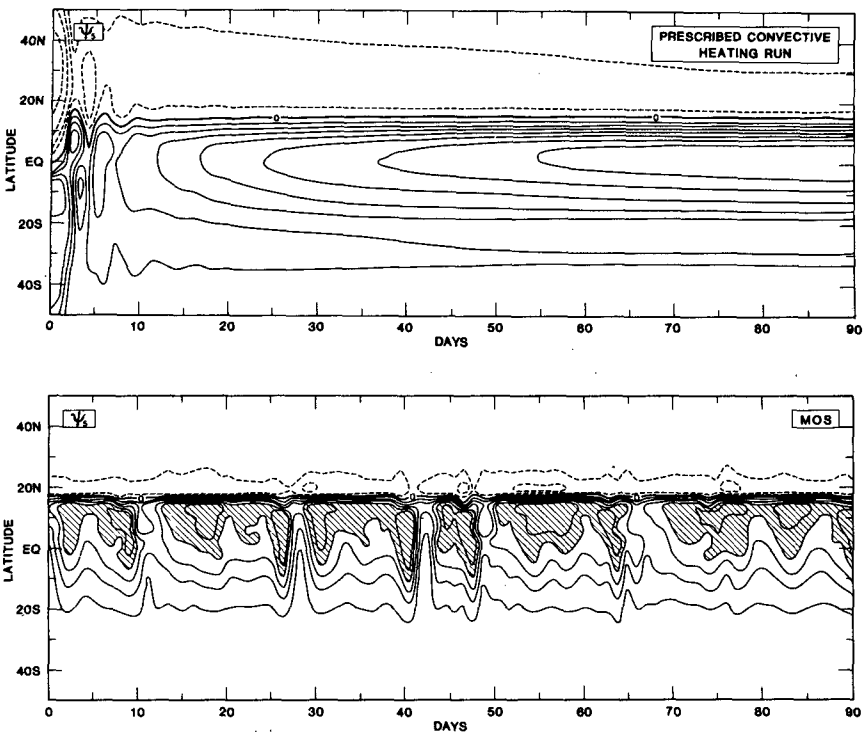

FIG. 3. Time series of ψ_5 for a run with prescribed latent heating (upper panel) and dynamically determined heating (lower panel) for the all-ocean summer run (MOS). Units 10^{10} kg s^{-1}.

northward propagation from the Southern Hemisphere is more intense and continues up to about 20°N in the summer run (Fig. 4). In this run, north of 20°N, the wave perturbation shows a stationary character. In the permanent equinox run, the speed of propagation both from south to north and north to south is about 1° latitude per day. In the permanent solstice run the speed of propagation of the northward movements of this perturbation is about 1.5° latitude per day.

2) VARIABLE SOIL MOISTURE RUN—PERMANENT SUMMER SOLSTICE

In the two runs described in the previous section, the soil moisture was held fixed. The run described with sun fixed over 23.5°N, was repeated letting the soil moisture interact with the hydrology (experiment V). As in the fixed soil moisture experiments, a climatological distribution of moisture was prescribed for the radiative calculations which was held constant with time. Thus a new feedback mechanism was introduced in this run. The model was again integrated for about 150 days and we examined the time evolution of precipitation, surface air temperature, the streamfunction at level 5 and the one at level 2 for the last 90 days of integration. It was seen from the temperature field as well as the precipitation field that the clear northward propagation seen in the fixed soil moisture run was not seen very clearly in this run. There were, however, signs of weak northward propagation between 10°S and 20°N. We also noted from the temperature field that the surface temperatures in the Southern Hemisphere tropics and subtropics between the equator and 30°S were higher in this case as compared to the fixed soil moisture case. Similarly, the surface temperatures in the subtropics and middle latitudes in the Northern Hemisphere were higher for this run as compared to the fixed soil moisture run. This is due to the fact that our model tends to dry out the land in the descending branches of the Hadley cells. Although the northward propagation of the wave perturbation in the lower atmosphere as seen in the fixed soil moisture run was not very clearly seen for the variable soil moisture run, it was seen from the streamfunction fields for this run that the Hadley circulation still showed the strong and weak episodes. The changes in the surface fluxes in the variable soil moisture run are very much dependent on how the surface processes are parameterized. It is seen that the parameterization of the surface processes in the GLAS Climate Model tends to make the land unrealistically dry or unrealistically wet. This is why the propagation characteristics seen in the fixed soil moisture run were not clearly seen in the variable soil moisture run. As this run does not add any new information but qualitatively shows the

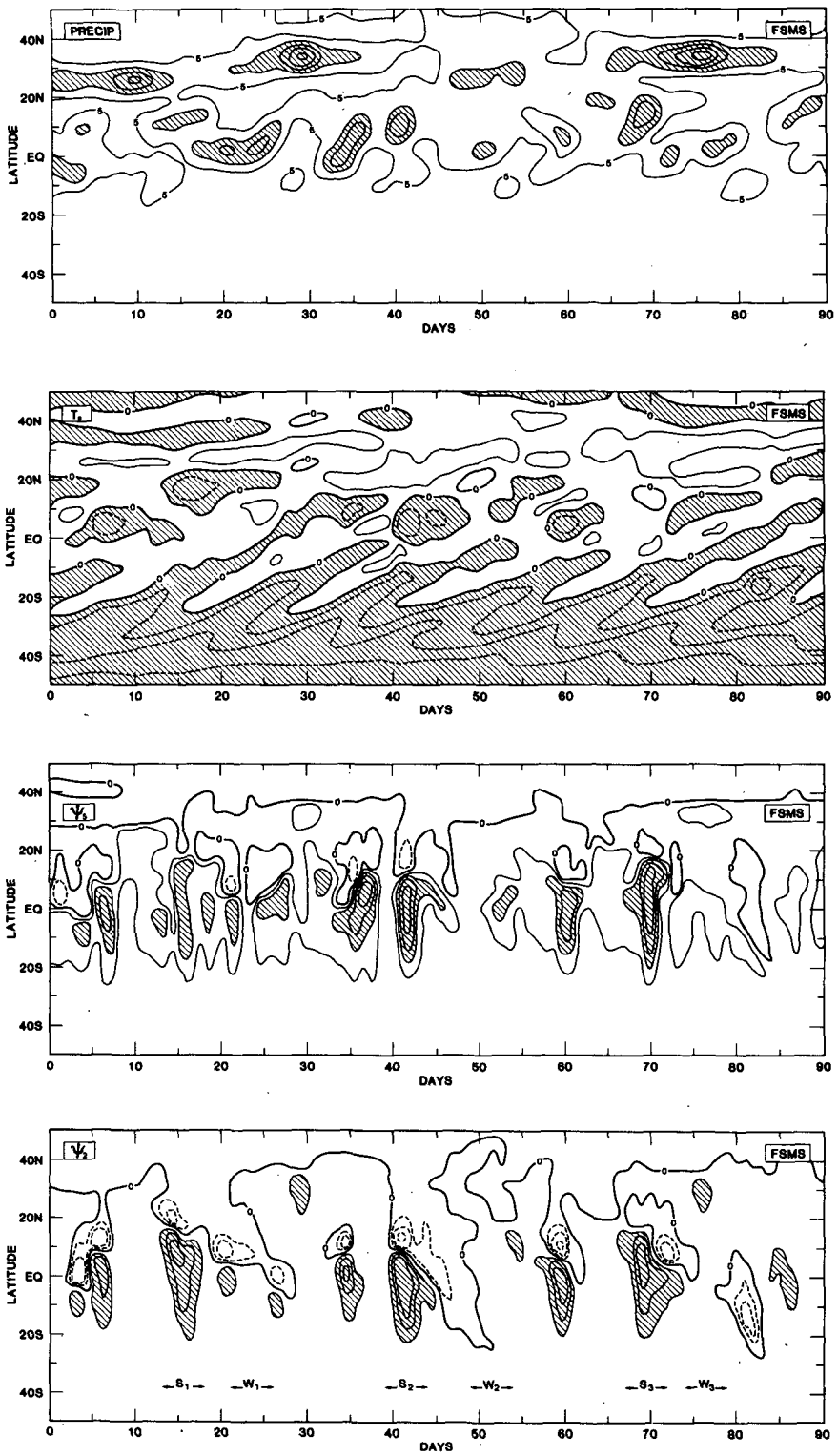

FIG. 4. As in Fig. 2 but for the fixed soil moisture, summer (FSMS) run. A unit of 300 is subtracted from the *TS* field and negative areas are shaded. Contour interval for *TS* and *P* is 10, and that for ψ_5 is 25. For ψ_2, negative contour interval is 10 and positive contour interval is 20. For *P*, contours greater than 15 are shaded, for ψ_5 contours greater than 50 are shaded while for ψ_2, contours greater than 20 are shaded.

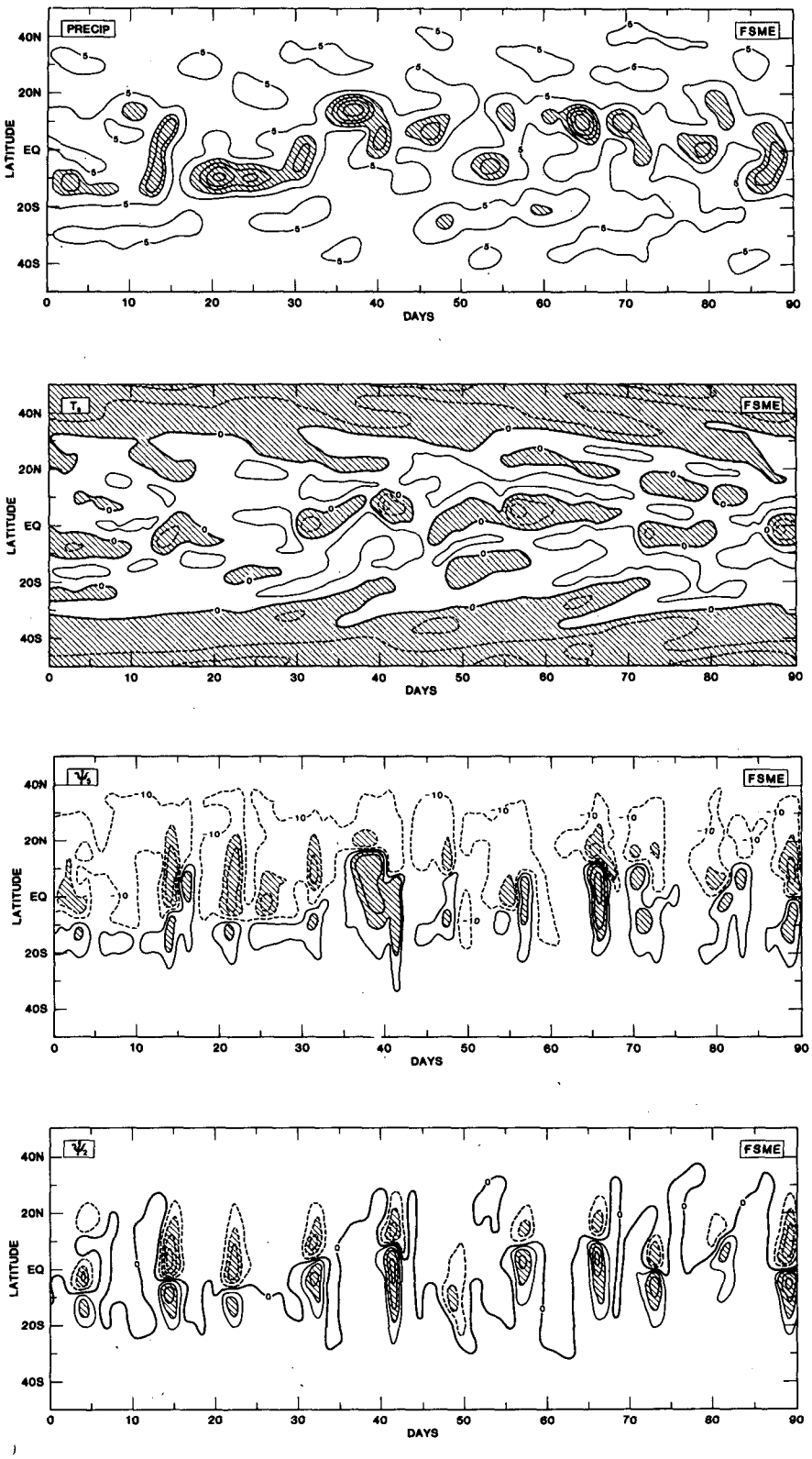

FIG. 5. As in Fig. 2 but for the fixed soil moisture, equinox (FSME) run. Contour interval for P and TS is 10, that for ψ_5 is 30 and that for ψ_2 is 20. For ψ_5, contours greater than 40 are shaded, for ψ_2, contours greater than 20 are shaded.

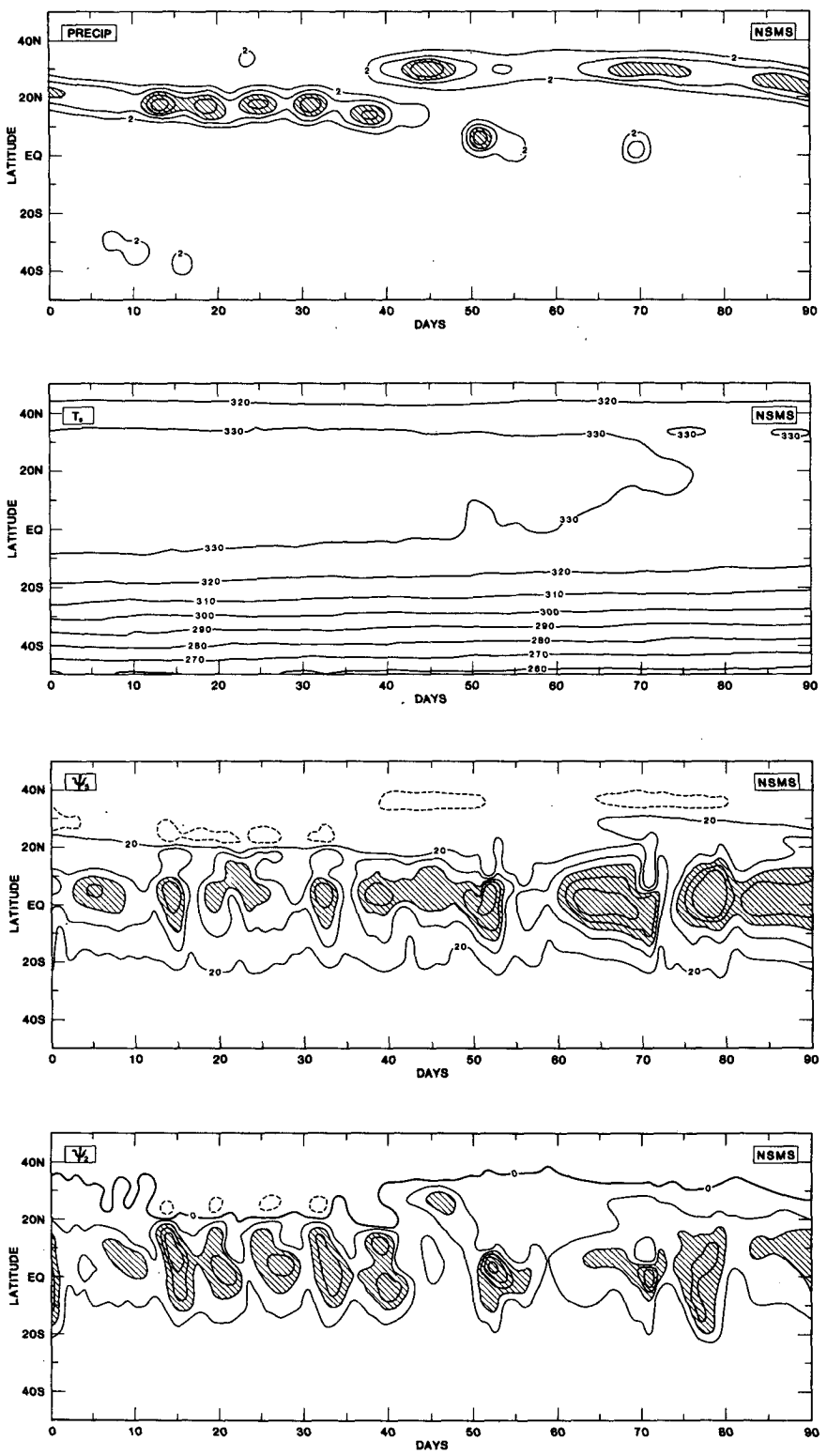

FIG. 6. As in Fig. 2 but for the no surface evaporation, summer (NSMS) run. The contour interval for *TS* is 10, that for *P* is 3, for ψ_5 is 30 and that for ψ_2 is 10. For *P*, contours greater than 8 are shaded, for ψ_5 contours greater than 80 are shaded and for ψ_2, contours greater than 20 are shaded.

same episodic behavior of the Hadley circulation, we shall not present the time series of various quantities for this run.

3) NO SURFACE EVAPORATION RUN—PERMANENT SUMMER SOLSTICE

In order to examine the role of land surface evaporation we carried out one experiment corresponding to the permanent summer solstice condition in which there was no evaporation from land, which is equivalent to assuming that the soil was dry and kept dry (experiment VI). At the initial time a moisture distribution was prescribed for the atmosphere. The model was again integrated for about 150 days and the temporal evolution of the precipitation field, the surface air temperature, the streamfunction at level 5 and the one at level 2 for the last 90 days are shown in Fig. 6. The surface temperatures for the dry land is much higher than those for the wet land (Fig. 4). We also note that the surface temperature does not show the wave structure in the north–south direction and in particular, it does not show the northward propagation. The precipitation results from the initial moisture in the atmosphere which is converged at the ascending branch of the Hadley cells. As time progresses this moisture precipitates out and the precipitation tends to die down. This is seen from the gradual weakening of the precipitation field. However, it is interesting to note that as long as some moisture exists in the atmosphere and hence moist convective activity, there exists the strong and weak episodes of the circulation. This is seen from the precipitation field as well as the streamfunction fields.

3. Further analysis of the results and discussions

In the previous Section we have presented results which show that moist convection and land surface processes result in two interesting phenomena in the model tropical atmosphere. First, it gives rise to episodes of strong and weak Hadley circulations in the atmosphere. In the vertical this behavior is seen from the lower atmosphere all the way to the upper troposphere. The atmosphere exhibits this behavior whenever the moist convective heating is determined by dynamics and is independent of whether the lower boundary is land or ocean. If the lower boundary is wet land, however, a wavy structure in the north–south direction is superimposed on the basic oscillation of the circulation in time. This wave perturbation is confined to the lower atmosphere (prominent up to about 850 mb) and propagates to the position of maximum radiative heating. This phenomenon of wave propagation in the lower atmosphere is not seen if the lower boundary is dry land. On the basis of these preliminary evidences we propose the following hypothesis as to the origin of these two phenomena. First, the basic oscillation (the episodic behavior) of the circulation results due to interactions between moist convective and dynamical processes. As the convection proceeds, it makes the atmosphere conditionally neutral and slows down the moist convective activity. Then the dynamics brings the atmosphere back at a still later time to be conditionally unstable. As the strength of the Hadley circulation depends strongly on the latent heating, the Hadley circulation also oscillates with the moist convective activity. Second, we propose that the wave propagation in the north–south direction is basically controlled by the fluctuations in the latent heat flux from the surface (surface evaporation).

In the following two subsections, we shall study the two phenomena discussed above in some more detail and present more evidence supporting the hypothesis presented above regarding their origin.

a. Spectral and band-pass filter analysis of the results

From Figs. 2–5, it is seen that the oscillations of the circulation have a period in the range of 10–20 days in the tropics. In order to examine the dominant periodicities, we carried out spectral analysis of the various fields using a daily averaged output for 120 days. It is seen from this analysis that there are two dominant periodicities, one with period between 10–15 days and another with period between 20–40 days. As an example, we present the spectral analysis of the precipitation field at 26 and 10°N for the fixed soil moisture run corresponding to permanent summer solstice (FSMS run) in Fig. 7. We would like to emphasize, however, that the amplitude of these oscillations are seen to vary by a certain amount depending on which field we examine at which latitude belt. We examined various fields at various latitude belts and found that the qualitative features depicted by Fig. 7 remain the same.

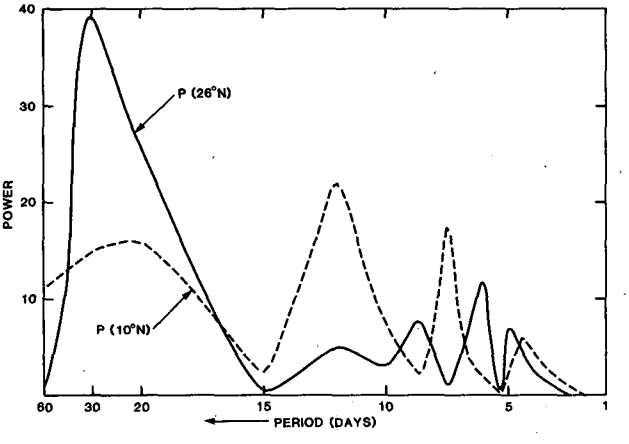

FIG. 7. Spectral analysis of precipitation for the fixed soil moisture, summer run at 26 and 10°N.

In order to study the circulation within these two frequency domains we designed two band pass filters. These are second-order Butterworth filters similar to one used by Murakami (1979). As discussed by many authors (Murakami, 1979; Shank, 1967; Guilleman, 1957), the Butterworth filter has the advantage that it require weights extending to only few data points on either side of the central point. The response function for this filter is given by

$$W(z) = \frac{a(1 - z^2)}{1 + b_1 z + b_2 z^2}, \quad (1)$$

where $W(z)$ is the response function, $z = \exp(-i\omega\Delta T)$, where ω is the frequency and ΔT is the sampling interval. The constants a, b_1, and b_2 determine the sharpness of the filter. The response functions for the two filters used in this study are shown in Fig. 8. Filter 1 has maximum response around a 12-day period while filter 2 has maximum response around a 30-day period. One half the maximum response occurs for filter 1 at periods 9.6 days and 15 days while that for filter 2 occurs at periods 20 days and 45 days.

We used these two band pass filters on various fields to examine how much of the basic oscillation of the circulation is contained within these two frequency domains. As an example, in Fig. 9 we present filtered streamfunction at level 2 (175 mb) for the fixed soil moisture summer run after using filter 1 and filter 2, respectively. It is seen that in both frequency domains, the circulation is stationary in the upper troposphere. We also examined (not shown here) the streamfunction at level 9 (945 mb) using these two filters. The filtered streamfunction at level 9 shows the propagating character in the lower troposphere. Moreover it is seen that the response in the 10–15 day period is stronger than that in the 20–40 day period. We examined various other fields using these two band pass filters. All the fields show the same behavior.

Earlier in this section we proposed that the origin of these oscillations is due to convective–dynamical interactions. Evaporation and dynamical convergence of moisture give rise to moist convection. When moist convection persists for some time it brings the atmosphere to conditionally neutral regime and the moist convection slows down. Then the dynamics brings the atmosphere back to conditionally unstable regime at a later time. The dynamics may influence the moist convective activity in the tropical atmosphere in the following ways. In the ITCZ region, the heat released from the moist convective activity accelerates the Hadley circulation but convergence of the relatively dry air from the descending branch of the Hadley cell into the ITCZ region will tend to slow down the moist convective activity and hence the Hadley circulation. We also recall that the surface temperature at a given latitude shows an oscillating character (e.g. see Fig. 4). The evaporation which is related to the surface temperature also shows (not shown here) a similar oscillation with a period of roughly two weeks. The combined effect of these two mechanisms can give rise to alternate moist and dry regimes in the tropical atmosphere. We examined (not shown here) the time series of departure of the specific humidity field at various latitudes from the long term time mean at the same latitudes for the fixed soil moisture summer run (experiment III, FSMS run). At the lowest four model levels (945 mb, 835 mb, 725 mb and 615 mb respectively), this field shows clear episodes of moist and dry regimes. These moist and dry episodes are found to be in phase with the strong and weak phases of the Hadley circulation respectively.

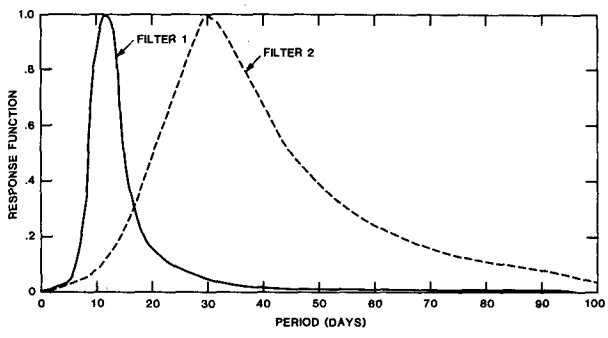

FIG. 8. The response functions for the two band pass filters used in this study.

Whether the oscillations of the moist convective activity are indeed due to the modification of the atmosphere stability because of the drying and moistening of the tropical atmosphere can be seen by examining the time evolution of the necessary condition for cumulus convection. Our model uses cumulus parameterization developed by Arakawa for the three level UCLA GCM but as modified and described by Somerville *et al.* (1974) for the use in a nine level model. As the main contribution to the convective precipitation comes from the deep convection, we shall examine only the *necessary* condition for deep convection. This condition in our model is given by

$$h_5 > h_3^* > h_1^*, \quad (2)$$

where $h = C_pT + gz + Lq$, $h^* = C_pT + gz + Lq^*$ are the moist enthalpy and saturation value of the moist enthalpy respectively. The subscripts 5, 3 and 1 refer to the central levels between level 8 and level 9, level 6 and level 7 and level 4 and level 5, respectively. We examined the time series of $h_5 - h_3^*$, $h_3^* - h_1^*$, etc., for the fixed soil moisture summer run and found that indeed there are regimes in time when the condition given by Eq. (2) is not satisfied. We also found that these regimes are in phase with the weak regimes of the circulation shown in Fig. 4. Thus, the oscillations

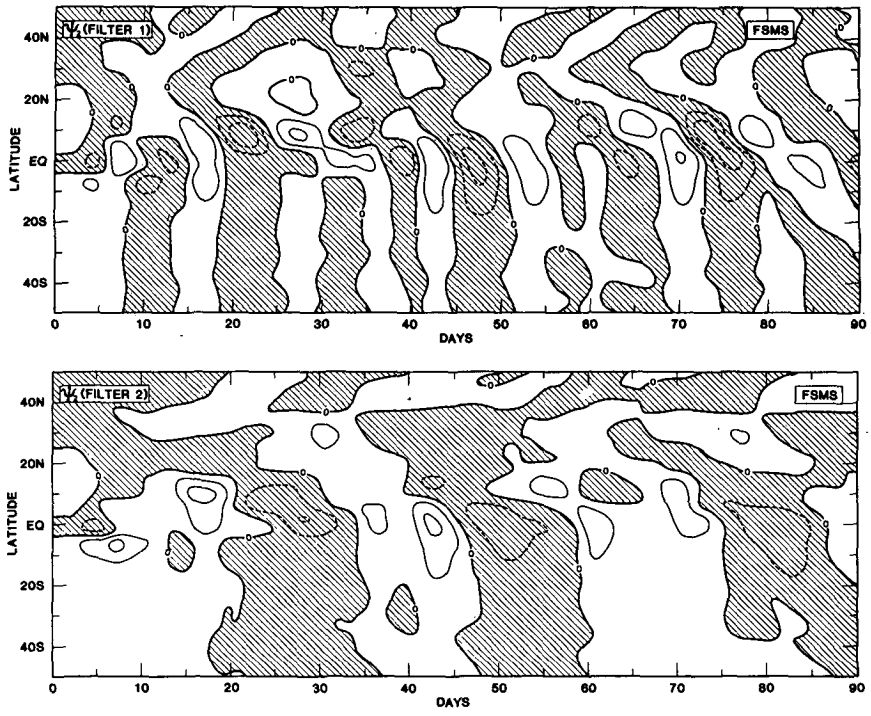

FIG. 9. Filtered ψ_2 for the fixed soil moisture, summer (FSMS) run after using filter 1 and filter 2 respectively. Negative areas are shaded. Units 10^{10} kg s^{-1}. Contour interval is 10.

of the moist convective activity are related to the changes in the moist stability which in turn are due to the moistening and drying of the tropical atmosphere.

The arguments presented above might explain why there are two dominant periodicities. An examination of the evaporation field shows that it oscillates with a period of approximately two weeks. Considering a representative Hadley cell of 20 degrees horizontal extent and with representative vertical velocities (90 mb day^{-1} in the ascending branch and 26 mb day^{-1} in the descending branch) and meridional velocities (3 m s^{-1} in the lower branch and 6 m s^{-1} in the upper branch), the excursion time of an air parcel in the Hadley cell can be calculated to be about 42 days. Thus, the 10–20 day oscillation may result from the oscillations in the evaporation from the surface while the 20–40 day oscillation may occur due to dry air convergence from the descending branch of the Hadley cell.

It may be argued at this point that a time series of 150 days is not sufficient to establish the existence of the 20–40 day oscillation. Therefore, we integrated the fixed soil moisture summer run (experiment III) for a total of 600 days and examined the time series of various fields. The examination of these long time series established the existence of the 20–40 day oscillation with greater confidence.

Regarding the propagation characteristics of the circulation in lower atmosphere, we noted earlier that it is not seen in the dry land case. Thus, it seems that the propagation characteristics in the lower atmosphere is controlled by the fluctuations in the land surface evaporation. In order to get further insight into this phenomenon, we present the time series of filtered (using filter 1) total precipitation, surface air temperature and net heat balance at the ground for the fixed soil moisture summer run in Fig. 10. We note that all three fields show significant northward propagation to about 20°N. It is seen that the surface temperature (TS) field lags behind the net heat balance at the ground by a couple of days but TS and precipitation are in phase. In other words, positive heat balance at the ground gives rise to higher surface temperature after a couple of days which in turn is related to increased precipitation. However, it is not clear from Fig. 10 which component in the heat balance at the ground has a dominant role. The net heat balance at the ground is given by

$$(\Delta T)_g = \text{net radiation} - SH - LH, \qquad (3)$$

where net radiation equals shortwave radiation minus longwave radiation, SH is sensible heat flux from the ground and LH the latent heat flux from the ground (evaporation). In order to examine which one of these components has a more dominating influence in determining the net heating at the ground, we plotted 3 day averages of these qualities for the fixed soil moisture case with permanent summer solstice. Three such con-

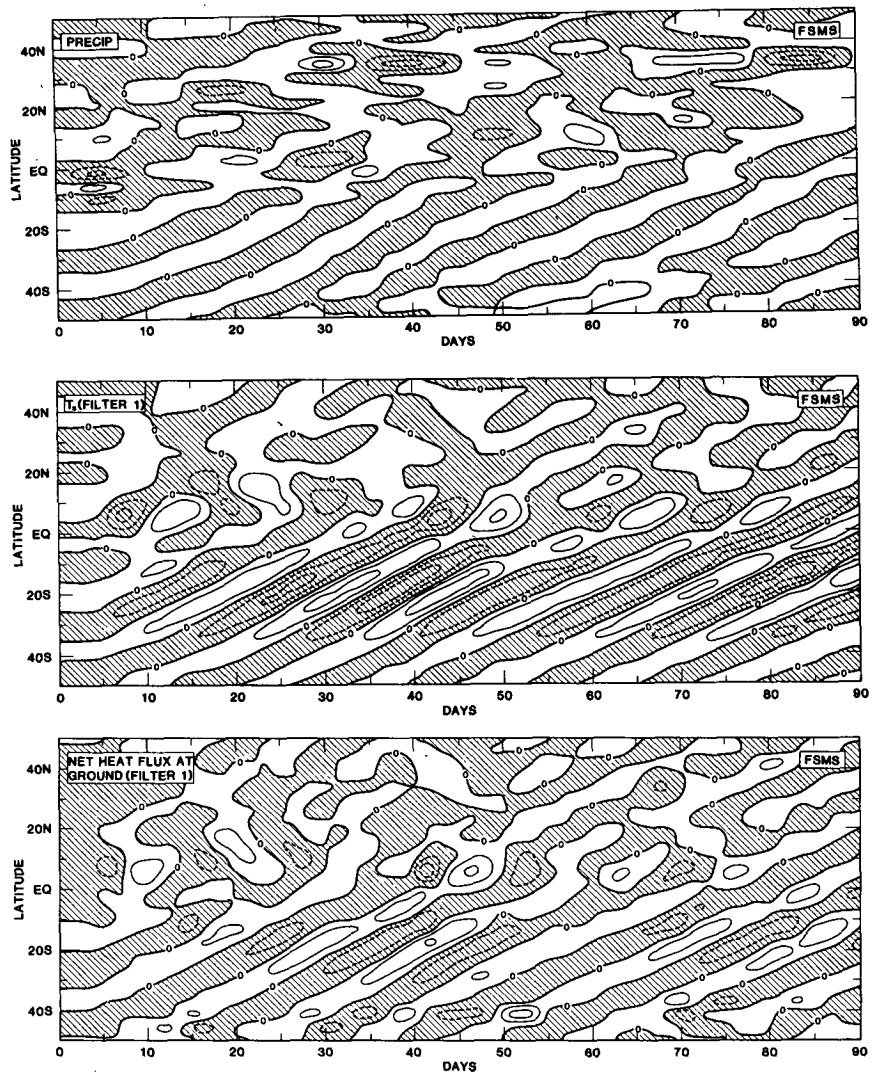

FIG. 10. Total precipitation, *TS*, net heat balance at the ground for the FSMS run after using filter 1. Negative areas are shaded. Contour interval for *TS* is 4, that for the net heat balance is 20 and that for precipitation is 10. Units for precipitation are mm day^{-1}, that for *TS* is °K, and for heat balance at ground it is Ly day^{-1}.

secutive plots of three day averages are shown in Fig. 11 starting with day 60 in the time series plots. It is seen from Fig. 11 that the fluctuations in the *LH* flux are larger than the corresponding fluctuations in the *SH* flux. Therefore, the *LH* flux (i.e. the surface evaporation) has a dominating influence in determining the surface heating or cooling. In general, large evaporation is associated with cooling of the surface and vice versa.

In order to examine the strength of the wave perturbation over the ocean as compared to that over the land, we used filter 1 on the surface air temperature for the all ocean summer run (experiment II). It was seen (not shown here) that the amplitude of the surface air temperature perturbation over the ocean was about 1°C as compared to 5–10°C over the land (Fig. 10). Thus, the wave perturbation in this frequency domain is stronger over the land as compared to that over the ocean.

b. *Vertical structure of the circulation during strong and weak epochs*

In the previous sections, we have clearly shown the episodic behavior of the Hadley circulation. In order to examine the vertical structure of the circulation during strong and weak regimes, we constructed composites for the two contrasting periods. This was done by taking the average of three 5-day periods of strong epochs and three 5-day periods of weak epochs. The

periods selected for the fixed soil moisture summer run for the strong epochs correspond to the periods S1, S2, and S3 shown in Fig. 4. Similarly, the periods selected to construct the composite for the weak epochs correspond to the periods shown by W1, W2 and W3 in Fig. 4. The streamfunction, the zonal wind and the temperature for the corresponding weak epochs for the fixed soil moisture summer run are shown in Fig. 12. The same quantities corresponding to the strong epochs for this run are shown in Fig. 13.

From Figs. 12 and 13 it is seen that there exists a remarkable difference between the streamfunction fields during the two epochs. In particular, during strong epochs, the ITCZ is around 18°N while during the weak epochs the ITCZ is around 5°N. Moreover, the ITCZ is much stronger during the strong epochs, compared to the same during the weak epochs. Moreover, the maximum mass flux in the Hadley circulation increases by more than a factor of two during strong regimes as compared to that during weak regimes.

The zonal winds show that neither the position nor the strength of the subtropical jets change significantly during the two regimes. However, the strength of the tropical easterlies in the upper level is increased during strong episodes as compared to those during weak episodes. On the other hand, the upper level easterlies in the subtropics between 20–30°N is reduced in strength during strong episodes as compared to those during weak episodes.

The temperature field does not show large changes in the upper atmosphere during the two episodes. In the lower atmosphere the temperatures are increased between 20 and 40°N during weak episodes as compared to those during strong episodes. This seems to be due to the adiabatic compression associated with the sinking branch in this region seen during weak episodes.

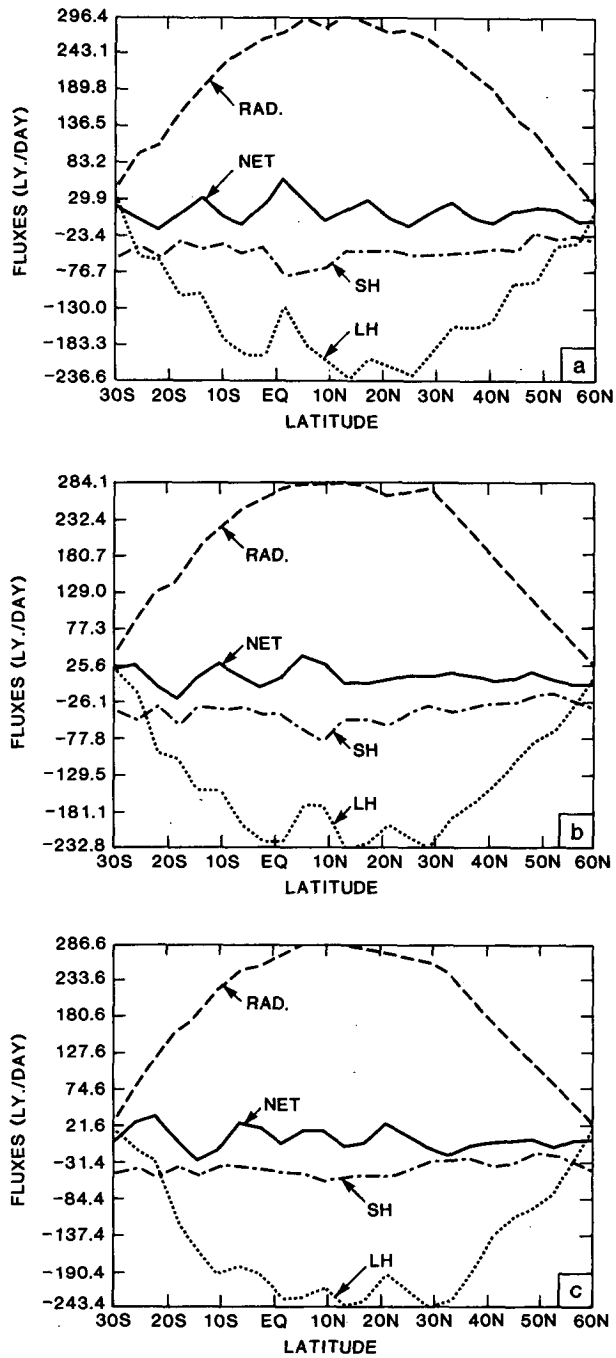

FIG. 11. Three consecutive 3-day averages of the components for the surface heat balance for the fixed soil moisture, summer run. All quantities are in units of Ly day^{-1}. In order to show the fluctuations in all the components clearly using the same scale, a unit of 250 Ly day^{-1} is subtracted from the net radiation field while it is added to the *LH* field.

4. Summary and conclusions

We carried out several long time integrations with a symmetric version of the GLAS Climate Model with hydrology and with either all ocean or all land lower boundary. This model discussed in detail in GSSS, has realistic parameterizations for the radiative, convective and surface processes. The model uses σ-coordinate with nine levels in the vertical and a 4° latitude grid in the north–south direction. Examination of the time evolution of the tropical circulation reveals two interesting phenomena.

First, the streamfunction fields show that the Hadley circulation in the tropics has strong and weak episodes. This episodic behavior of the Hadley circulation occurs whenever there is moisture in the atmosphere that interacts with the dynamics to produce convection no matter whether the lower boundary is land or ocean. Second, surface temperature, precipitation and streamfunction fields in the lowest model layers show a wave phenomenon with a length scale of about 15–20 degrees latitude in the north–south direction. This

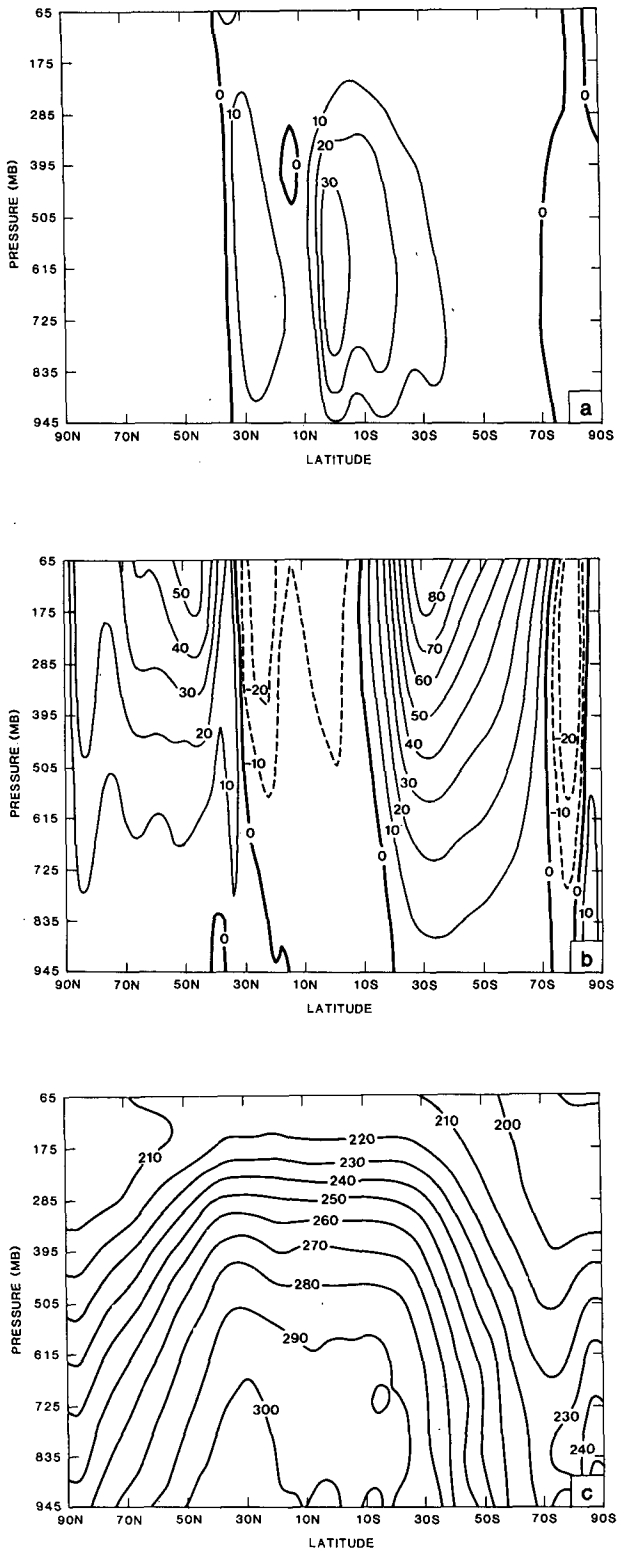

FIG. 12. Composite vertical structure of the streamfunction, the zonal wind, and the temperature for the weak epochs, the fixed soil moisture summer run. a) Streamfunction, contour interval 10×10^{10} kg s^{-1}. b) Zonal winds, contour interval 10 m s^{-1}. c) Temperature, contour interval, 10K.

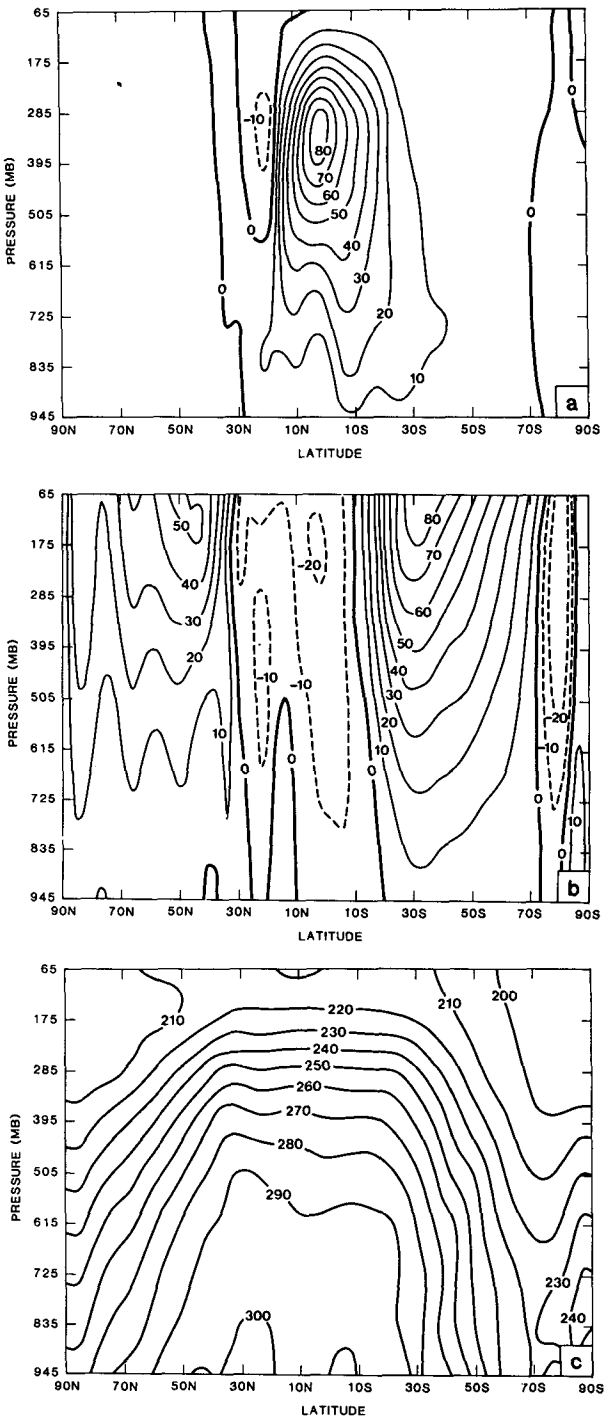

FIG. 13. As in Fig. 12 corresponding to the strong epochs.

wave seems to propagate to the region of maximum radiative heating.

As mentioned in the Introduction, observational analyses (Yasunari, 1979, 1981; Sikka and Gadgil, 1980) have revealed that there are two dominant periodicities in the tropics and subtropics during Northern Hemisphere summer—one with a period between 10

and 20 days and another with a period between 30 and 50 days. Using two band pass filters with maximum response centered around these two ranges of frequencies, Yasunari (1980) showed that the filtered geopotential height at 850 mb has a northward propagating character while that at 200 mb has more or less a stationary character. These studies also indicate that one phase of both these oscillations are related to weak monsoon activity (breaks) while the other phase is related to strong monsoon activity (active phase). Thus there is some evidence that the "active" and "break" phases of the South Asian monsoon are related to these basic oscillations of the tropical atmosphere.

With our zonally averaged model, we indeed find two dominant periodicities in the tropics and subtropics during Northern Hemisphere summer. One of these oscillations has period between 10 and 20 days while the other has period between 20 and 40 days. As seen by Yasunari (1979) from the study of the cloudiness fluctuation, we find that the 20–40 day period is dominant in the Northern Hemisphere subtropics. Moreover, our model also shows the northward propagation of these fluctuations in the lower atmosphere.

On the basis of our results we put forward the following hypothesis regarding the origin of the basic oscillation of the Hadley circulation. We propose that it results from a convective dynamical feedback process. This is supported by the fact that if the convective heating field for the atmosphere is prescribed and held constant in time, this oscillation is not seen. We believe that once moist convection takes place in the tropical atmosphere, and maintains for some time, the static stability of the atmosphere changes in such a way that at a later time it becomes moist convectively neutral and slows the convective activity. Then dynamical and radiative relaxation brings the atmosphere at a still later time to nearly the original convectively unstable situation when moist convection reactivates again. We examined the condition for moist convection by looking at the time series of moist enthalpy at various model levels. It was found that the model tropical atmosphere goes through periods of conditionally stable and unstable regimes. We also found that these changes in the stability are related to moist and dry spells of the tropical atmosphere. Thus, the quasi-periodic oscillations of the Hadley circulation which result from oscillations of the latent heating field can be traced to the moistening and drying of the tropical atmosphere.

Yasunari (1981) suggested that the 40-day oscillation in the Asian monsoon region is a forced oscillation due to the periodic cold air outbreaks from the Southern Hemisphere. We agree that in the real atmosphere, a part of the response to the 40-day oscillation may come from such a forced motion. However, we have shown that convective–dynamical feedback inherent in the tropics alone can give rise to such oscillations.

In the lower atmosphere, the surface temperature and the precipitation field show a wave phenomenon. This wave perturbation has a scale of about 15–20° latitude in the north–south direction. This wave perturbation also seems to move toward the position of the maximum radiative heating. For the equinox condition, when the sun is over the equator, it moves north toward the equator from the Southern Hemisphere while it moves south toward the equator from the Northern Hemisphere. For the summer solstice condition, it moves northward from the Southern Hemisphere up to about 20°N. North of 20°N in this case, it shows a stationary behavior. We have shown that the amplitude of this wave perturbation is large over the land and small over the ocean. The streamfunction fields at 505 mb and 175 mb show that this perturbation is essentially confined to the lower atmosphere.

As for the origin of the wave phenomenon in the lower atmosphere, we propose that it is maintained by the latent heat of evaporation from the surface. We examined the different components of the surface heat balance and found that the fluctuation in the latent heat of evaporation is the dominant factor in determining the fluctuations of the net heat balance at the surface. Our hypothesis is also supported by the fact that the amplitude of this oscillation is large over land and small over the oceans. This is because, evaporation can change the surface temperature over the land drastically while it can only have weak influence on the surface air temperature over the ocean. Our hypothesis is further supported by the fact that for the experiments where land was kept dry this wave phenomenon in the lower atmosphere is not seen.

In the Introduction and earlier in this section we have noted that these results from our numerical simulation have important relevance to several observations. We would like to emphasize that although most of the observational studies referred to earlier use only station data or data averaged over a region, it is interesting that quite similar results are seen with a zonally averaged general circulation model.

In Part I and in Section 2 of this paper we have discussed the reason for suppressing the cloud–radiation feedback in our symmetric model. Inclusion of a realistic representation of this process (allowing for fractional cloudiness) in the model may result in an additional source of oscillation in the model tropical atmosphere. Finally, we would like to point out that the phenomena discussed in this model study depend on the particular parameterizations of various physical processes used in our model, and therefore, more numerical experiments with other parameterizations and models should be done to establish the validity of the hypothesis based on the present limited study.

Acknowledgments. The authors would like to thank Dr. Milton Halem for his encouragement throughout this work. We would also like to thank Drs. David

Randall and Richard Wobus for their comments on a previous version of this manuscript. Thanks are also due to Laura Rumburg for drafting the figures, Mary Ann Schaefer for typing the manuscript, and Lena Fornito for helping in the diagnostic analysis of the results. The work of one of the authors (BNG) was supported in parts by National Research Council, Washington, D.C. and Universities Space Research Association, Columbia, MD.

REFERENCES

Anderson, J. R., and R. D. Rosen, 1983: The latitude height structure of 40–50 day variations in atmospheric angular momentum. *J. Atmos. Sci.*, **40,** 1584–1591.

Goswami, B. N., J. Shukla, E. K. Schneider and Y. C. Sud, 1984: Study of the dynamics of the Intertropical Convergence Zone with a symmetric version of the GLAS Climate Model. *J. Atmos. Sci.*, **41,** 5–19.

Guillemin, E. A., 1957: *Synthesis of Passive Networks.* Wiley and Sons, 599–609.

Keshavamurty, R. N., 1973: Power spectra of large scale disturbances of the Indian South West monsoon. *Indian J. Meteor. Geophys.*, **24,** 117–124.

Krishnamurti, T. N., and H. N. Bhalme, 1976: Oscillations of a monsoon system. Part I: Observation aspects. *J. Atmos. Sci.*, **33,** 1937–1954.

——, and P. Ardanuy, 1980: The 10 to 20 day westward propagating mode and "Breaks in the Monsoons". *Tellus,* **32,** 15–26.

——, and D. Subrahmanyam, 1982: The 30–50 day mode at 850 mb during MONEX. *J. Atmos. Sci.*, **39,** 2088–2095.

Madden, R. A., and P. R. Julian, 1971: Detection of a 40–50 day oscillation in the zonal wind in the tropical Pacific. *J. Atmos. Sci.*, **28,** 702–708.

——, and ——, 1972: Description of global scale circulation cells in the tropics with 40–50 day period. *J. Atmos. Sci.*, **29,** 1109–1123.

Murakami, M., 1976: Analysis of summer monsoon fluctuations over India. *J. Meteor. Soc. Japan,* **54,** 15–31.

——, 1979: Large scale aspects of deep convective activity over the GATE area. *Mon. Wea. Rev.*, **107,** 994–1013.

Shank, J., 1967: Recursion filters for digital processing. *Geophysica,* **32,** 32–51.

Sikka, D. R., and S. Gadgil, 1980: On the maximum cloud zone and the ITCZ over Indian longitudes during the South West monsoon. *Mon. Wea. Rev.*, **108,** 1840–1853.

Sommerville, R. C. J., P. H. Stone, M. Halem, J. E. Hansen, J. S. Hogan, L. M. Druyan, G. Russel, A. A. Lacis, W. L. Quirk and J. Tenenbaum, 1974: The GISS model of the global atmosphere. *J. Atmos. Sci.*, **31,** 84–117.

Stevens, D. E., 1983: On symmetric stability and instability of zonal mean flows near the equator. *J. Atmos. Sci.*, **40,** 882–893.

Webster, P. J., and L. C. Chou, 1980a: Seasonal structure of a simple monsoon system. *J. Atmos. Sci.*, **37,** 354–367.

——, and ——, 1980b: Low-frequency transitions of a simple monsoon system. *J. Atmos. Sci.*, **37,** 368–382.

Yasunari, T., 1979: Cloudiness fluctuations associated with the Northern Hemisphere summer monsoon. *J. Meteor. Soc. Japan,* **57,** 227–262.

——, 1980: Quasi-stationary appearance of 30–40 day period in the cloudiness fluctuations during summer monsoon over India. *J. Meteor. Soc. Japan,* **58,** 225–229.

——, 1981: Structure of an Indian summer monsoon system with around 40-day period. *J. Meteor. Soc. Japan,* **59,** 336–354.